JOURNAL OF BACTERIOLOGY, June 1995, p. 3269–3276 Vol. 177, No. 11
0021-9193/95/$04.00+0

Disruption of a Gene Encoding a Novel Thioredoxin-Like Protein Alters the Cyanobacterial Photosynthetic Apparatus†

JACKIE L. COLLIER[1] AND ARTHUR R. GROSSMAN[2]*

Department of Plant Biology, Carnegie Institution of Washington, Stanford, California 94305,[2] and Marine Biology Research Division, Scripps Institution of Oceanography, University of California–San Diego, La Jolla, California 92093-0202[1]

Received 14 September 1994/Accepted 6 March 1995

A gene that may encode a novel protein disulfide oxidoreductase, designated *txlA* (thioredoxin-like), was isolated from the cyanobacterium *Synechococcus* sp. strain PCC7942. Interruption of *txlA* near the putative thioredoxin-like active site yielded cells that grew too poorly to be analyzed. In contrast, a disruption of *txlA* near the C terminus that left the thioredoxin-like domain intact yielded two different mutant phenotypes. One type, designated txlXb, exhibited a slightly reduced growth rate and an increased cellular content of apparently normal phycobilisomes. The cellular content of phycobilisomes also increased in the other mutant strain, designated txlXg. However, txlXg also exhibited a proportionate increase in chlorophyll and other components of the photosynthetic apparatus and grew as fast as wild-type cells. Both the txlXb and txlXg phenotypes were stable. The differences between the two strains may result from a genetic polymorphism extant in the original cell population. Further investigation of *txlA* may provide new insights into mechanisms that regulate the structure and function of the cyanobacterial photosynthetic apparatus.

The conversion of light energy into chemical energy (ATP) and reducing power (NADPH) by oxygen-evolving photosynthetic organisms requires the coordinated activity of photosystem I (PSI) and photosystem II (PSII), along with their light-harvesting antenna pigments and intermediary electron transport components. NADPH is produced only by linear electron flow through both PSII and PSI, but ATP can be produced either by linear electron flow or by cyclic electron flow around PSI alone (24, 34). In cyanobacteria, PSI is excited almost entirely by light absorbed by chlorophyll *a* (Chl; A_{max}, 440 and 680 nm), while PSII receives most of its excitation energy from light absorbed by the phycobilisomes (PBS; A_{max}, 560 to 620 nm [32]). Within these basic functional constraints, the structure of the photosynthetic apparatus is dynamic. For example, while the PBS-to-Chl ratio generally reflects the PSII-to-PSI ratio, under some conditions cyanobacteria can modulate the light-harvesting capacity of PBS relative to Chl independently of the PSII-to-PSI ratio by changing the size of the PBS (11, 20, 40) or the number of PBS relative to PSII (42). Cyanobacteria grown in light that is harvested primarily by PBS show a decline in the PSII-to-PSI ratio, while those grown in light harvested primarily by PSI show the opposite response (1, 26, 41, 44). These changes may allow cyanobacteria to balance the production of ATP and NADPH despite conditions favoring the activity of one photosystem over the other (26, 43). Carbon-limited cyanobacteria show a decline in the ratio of PSII to PSI that may reflect an increase in cyclic relative to linear photosynthetic electron flow. This change could increase the production of ATP relative to NADPH and help meet the extra demand for energy incurred by cells that must actively take up inorganic carbon (36, 45, 51, 53). Patterns of electron transport are also altered when cells are deprived of nitrogen or sulfur; PSI remains active despite complete degradation of the PBS and a dramatic decline in the activity of PSII (19).

The molecular mechanisms that underlie these modifications of the structure and function of the photosynthetic apparatus in response to metabolic and environmental cues are largely unknown. In both plants and cyanobacteria, the redox state of the cytochrome b_6f complex is believed to be involved in regulating the distribution of harvested light energy between the two photosystems in the short term via state transitions (3, 13, 47, 57) and in the long term through changes in the stoichiometry of the reaction centers (25, 37, 44, 48). A number of other photosynthetic and nonphotosynthetic metabolic processes in cyanobacteria may also be redox regulated (4, 12, 15, 56). However, the only reasonably well understood example of redox regulation in photosynthesis is the role that thioredoxins play in coordinating the activities of metabolic enzymes with the redox state of the photosynthetic electron transport system (14, 46). Thioredoxins are small, cytoplasmically localized members of a family of enzymes known as protein disulfide oxidoreductases (PDOs) that function by using their dicysteinyl active site to alter the redox state of other proteins (8, 23).

In this paper, we describe the isolation and characterization of a gene, designated *txlA* (thioredoxin-like), that encodes a protein exhibiting significant sequence similarity to the thioredoxins and to another group of PDOs, the protein disulfide isomerases (PDIs). The data presented here suggest that TxlA is involved, either directly or indirectly, in redox regulation of the structure and function of the cyanobacterial photosynthetic apparatus.

MATERIALS AND METHODS

Strains and culture conditions. *Synechococcus* sp. strain PCC7942 was cultured on both liquid and solid BG-11 medium as described previously (5, 17). In liquid medium, cultures were grown at 32°C with a light intensity of 50 μmol of photons m^{-2} s^{-1} (from three 40-W incandescent bulbs) and bubbled with air enriched to 3% CO_2. When appropriate, ampicillin was included at a concentration of 1.5 μg/ml, and spectinomycin was included at a concentration of 25 μg/ml in solid medium or 5 μg/ml in liquid medium.

Nucleic acid manipulations. All DNA and RNA techniques were performed according to standard procedures and as described previously (7, 18, 55). The

* Corresponding author. Phone: (415) 325-1521. Fax: (415) 325-6857.

† CIW/DPB publication no. 1207.

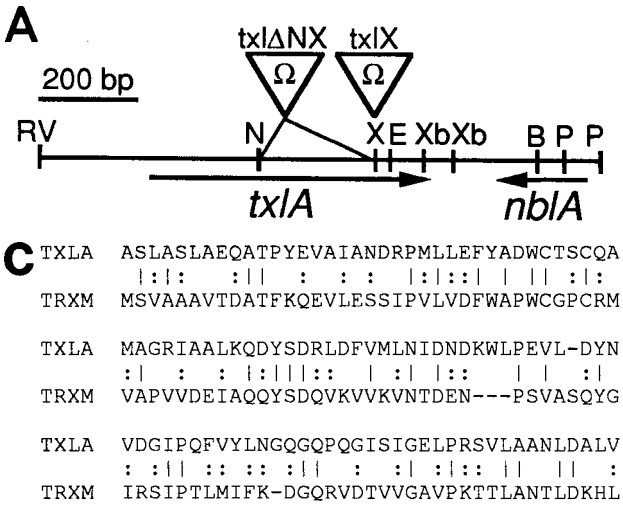

FIG. 1. Restriction map, nucleotide sequence, and similarity to thioredoxins of the region encoding *txlA*. (A) Map of the 1.2-kbp DNA fragment containing *txlA* and *nblA*. The locations and directions of the genes are indicated by large arrows below the map. The restriction sites are abbreviated as follows: B, *Bgl*II; E, *Eco*RI; RV, *Eco*RV; N, *Nco*I; P, *Pst*I; Xb, *Xba*I; X, *Xho*I. Also indicated are the modifications introduced into this region in the construction of plasmids ptxlΔNX, which replaces 250 bp of *txlA* with the Ω cassette encoding spectinomycin resistance, and ptxlX, which simply inserts the Ω cassette near the end of *txlA*. (B) Sequence of the *txlA* region from the *Eco*RV to the *Bgl*II site. The restriction sites underlined are as follows: bp 1, *Eco*RV; bp 452, *Nco*I; bp 701, *Xho*I; bp 718, *Eco*RI; bp 798 and 863, *Xba*I; and bp 1039, *Bgl*II. The amino acids in the hydrophobic region of the polypeptide (residues 14 to 31) are also underlined. The potential ribosome-binding site and the two cysteines of the putative active site are thickly underlined. (C) Alignment of residues 38 to 147 of TxlA with TrxM from *Synechococcus* sp. strain PCC7942 (46). Vertical lines indicate identical residues, and colons indicate conservative substitutions (PAM250 score, >0).

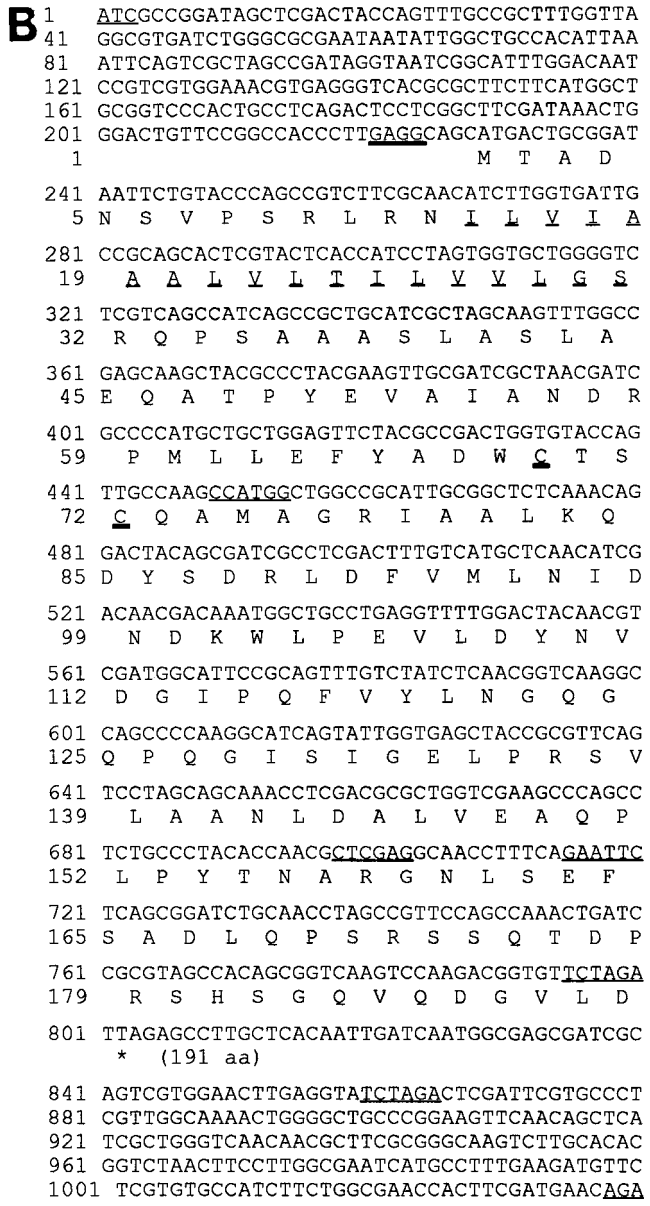

txlA gene sequence has been submitted to GenBank (accession number U05044). Disruption of *txlA* in pUC118 by interposon mutagenesis was performed by insertion of the *aadA* gene, which confers spectinomycin resistance (the Ω cassette [54]), into the *txlA* gene at two different sites. As diagrammed in Fig. 1A,pick;0126f1b;0;1;0 replacement of the 250-bp *Nco*I-*Xho*I fragment (from the *Nco*I site at bp 452 to the *Xho*I site at bp 718; see Fig. 1B) with the Ω cassette generated plasmid ptxlΔNX. A simple insertion of Ω into the *Xho*I site generated plasmid ptxlX. The plasmids were introduced into the cyanobacterium as described previously (38). Since pUC118 cannot replicate autonomously in cyanobacteria, only those cells in which the plasmid recombines into the cyanobacterial genome will grow on spectinomycin. Single homologous recombinants would be both ampicillin and spectinomycin resistant because of the integration of the entire plasmid into the chromosome. In double homologous recombinants, the endogenous *txlA* gene would be replaced by the plasmid-borne *txlA* gene that is interrupted by the Ω cassette, and the remainder of the plasmid would be lost. These cells would be spectinomycin resistant but ampicillin sensitive. In *Synechococcus* spp., double homologous recombination is generally far more common than single homologous recombination. Furthermore, each cyanobacterial cell carries multiple copies of the genome, so care must be taken to ensure that transformants contain a homogeneous complement of *txlA* loci.

The 1-kbp *Eco*RV-*Bgl*II fragment containing *txlA* was also subcloned into the shuttle vector pCB4′, which can replicate autonomously in both *Escherichia coli* and *Synechococcus* sp. strain PCC7942 (29), to generate plasmid ptxlA. The strand- and gene-specific RNA probe used to detect *txlA* mRNA was constructed by subcloning the 800-bp *Eco*RV-*Xba*I fragment, containing most of *txlA* and 230 bp of upstream sequence, into pBluescript KS^+. This construct (pJC39) was linearized with *Hin*dIII and transcribed in vitro with T7 RNA polymerase to generate a probe detecting only mRNA encoding TxlA (probe tT7).

Measurement of pigment content and photosynthetic activity. PBS and Chl concentrations were determined from whole-cell absorbance spectra with the equations of Arnon as described previously (6, 17). Growth rates were determined by measuring the rate of Chl accumulation during the logarithmic phase of growth, and culture densities were determined by counting cells in a hemacytometer. PBS were isolated and analyzed as described previously (16, 17). Oxygen evolution measurements were performed with a Clark-type O_2 electrode (Rank Brothers, Cambridge, United Kingdom) while the cells were illuminated at a saturating light intensity of 150 μmol of photons m^{-2} s^{-1} at 32°C in a water-jacketed cuvette.

The fluorescence emission spectra at 77 K of cyanobacterial cultures were measured with a Photon Technologies International (New Brunswick, N.J.) single-beam fluorometer as described previously (16, 19). The background fluorescence spectrum measured from sterile medium was subtracted from each sample spectrum, but no corrections were made for the spectral sensitivity of the instrument. The pairs of curves in each panel of Fig. 3 were normalized to each other at 650 nm.

A post hoc statistical analysis of the data was performed with either the Tukey honestly significant difference test of the SYSTAT package (1986; L. Wilkinson, Evanston, Ill.), when the number of values (n) was equal, or the Scheffe f test of the STATVIEW package (version 4.01; Abacus Concepts, Berkeley, Calif.), when n differed. For each characteristic (i.e., doubling time, PC/Chl ratio, phycocyanin [PC] per cell, Chl per cell, and rates of O_2 evolution), these analyses allowed the strains to be divided into two groups. All strains within group A were significantly different from those within group B, and the level of significance for those differing from the wild type is indicated in Tables 2, 3, and 4. For txlXg::ptxlA, analysis of both PC per cell and Chl per cell did not allow for classification into either group A or group B.

RESULTS

The *txlA* (thioredoxin-like) gene was cloned and sequenced because it lies immediately downstream of and in the opposite

TABLE 1. Results of three independent transformations of *Synechococcus* sp. strain PCC 7942 with plasmids ptxlΔNX and ptxlX

Plasmid and expt no.	No. of green colonies/no. of blue colonies (ratio)	No. of Amp^r colonies/total (% Amp^r)	
		Blue colonies	Green colonies
ptxlΔNX			
1	104/1,215 (0.083)	ND[a]	4/4 (100)
2	18/400 (0.045)	0/36 (0)	36/36 (100)
3	15/470 (0.032)	0/36 (0)	36/36 (100)
ptxlX			
1	ND	0/8 (0)	1/4 (25)
2	216/588 (0.367)	0/3 (0)	2/3 (67)
3	55/184 (0.30)	0/36 (0)	14/36 (40)

[a] ND, not determined.

orientation from *nblA*, a gene required for the degradation of PBS in nutrient-deprived *Synechococcus* sp. strain PCC7942 (18). We began investigating the function of *txlA* because antisense *txlA* transcripts (originating from *nblA*) are produced in nutrient-deprived cells, suggesting that changes in the expression of *txlA* may be involved in acclimation to nutrient-deficient conditions (16).

Sequence analysis. A restriction map of the region containing *txlA* is shown in Fig. 1A, and the DNA sequence between the *Eco*RV and *Bgl*II sites is presented in Fig. 1B. The *txlA* open reading frame initiates with a methionine that is preceded by a potential ribosome-binding site. The predicted molecular mass of TxlA is 21 kDa, with an isoelectric point (pI) of 4.2. The predicted protein is largely hydrophilic except for a domain of 18 hydrophobic residues (residues 14 to 31, underlined in Fig. 1B) near the N terminus. The TxlA sequence was used to search the GenBank database (Release 76). The 37 N-terminal and 44 C-terminal residues had no detectable similarity to any sequence in the database, but the central 110-residue region of TxlA exhibited significant similarity to a number of thioredoxins and PDIs. Alignment of TxlA with thioredoxin *m* (TrxM) of *Synechococcus* sp. strain PCC7942 (46) shows that the central region of TxlA is 29% identical and 60% conserved relative to TrxM (Fig. 1C). TxlA exhibits comparable levels of similarity to other thioredoxins and to the thioredoxin-like domains of PDIs (data not shown).

Genetic analysis. To investigate the function of *txlA*, the *txlA* region was cloned into pUC118, and a spectinomycin resistance cassette called Ω (see Materials and Methods) was inserted in vitro into the *txlA* open reading frame in two different positions (Fig. 1A). In the first of these constructs, designated ptxlΔNX, more than half of the thioredoxin-like region of the *txlA* open reading frame was removed and replaced with the Ω cassette. In the second construct, designated ptxlX, the Ω cassette was inserted into the *Xho*I site, which would cause a truncation of TxlA near the C terminus. If the normal function of TxlA requires that its thioredoxin-like domain be intact, replacement of normal *txlA* with the txlΔNX disruption should abolish TxlA activity. In contrast, the txlX disruption leaves the thioredoxin-like domain intact; it is less likely to have a severe effect on any PDO-like activity of TxlA.

Plasmids ptxlΔNX and ptxlX were introduced into wild-type *Synechococcus* sp. strain PCC7942, and transformants were selected on plates containing spectinomycin. The results of three separate transformations of wild-type *Synechococcus* sp. strain PCC7942 cultures with ptxlΔNX or ptxlX are summarized in Table 1. Two types of transformants were observed in each case. One colony type appeared blue and smaller than normal (blue colonies), while the other appeared similar to the wild type (green colonies). This would be expected if one type (i.e., blue colonies) resulted from the disruption of *txlA* by double homologous recombination, while the other (i.e., green colonies) resulted from single homologous integration of the plasmid into the genome generating both an intact and a disrupted copy of *txlA*. Following the introduction of ptxlΔNX, all of the green colonies were ampicillin resistant (single homologous recombinants), while all of the blue colonies were ampicillin sensitive (double homologous recombinants), as predicted. The blue colonies, designated txlΔNXb, grew very slowly on solid medium and died much more quickly than wild-type cells. We were only able to grow the txlΔNXb mutant in liquid medium twice. In both cases, a very long (7-day) lag period was observed, and the phenotypes of the two cultures were different. Therefore, the growth of txlΔNXb was greatly impaired by a loss of TxlA activity, and it is likely that the mutant strain only grew in liquid medium after the generation of secondary suppressor mutations. Hence, the txlΔNXb mutant was considered unreliable for further analysis.

In contrast to the results with ptxlΔNX, transformation with plasmid ptxlX yielded a much higher ratio of green to blue colonies (Table 1). All of the blue colonies were ampicillin sensitive, as expected for double homologous recombinants. However, approximately 60% of the green colonies were unexpectedly ampicillin sensitive; that is, they were also likely to be the consequence of double homologous recombination events. Hence, in this case, the true ratio of single to double recombinants was not equal to the ratio of green to blue colonies. If the ratio of single to double recombinants were calculated based on ampicillin sensitivity, it was approximately 0.1, which is more similar to the results for ptxlΔNX. Ampicillin-sensitive strains with the blue phenotype were designated txlXb, and ampicillin-sensitive strains with the green phenotype were designated txlXg. As shown in Southern analyses of genomic DNA (Fig. 2A), the 1.5-kbp *Eco*RI and 3.5-kbp *Pst*I fragments of wild-type cells increased in size to 3.5 and 5.5 kbp, respectively, in both the txlXb and txlXg mutants. The probe used included the region shown in Fig. 1A plus 800 bp upstream of *nblA*. These results demonstrated that both txlXb and txlXg contained the predicted disruption of *txlA* by the 2.0-kbp Ω cassette inserted at the *Xho*I site. Longer exposures confirmed that no uninterrupted copies of *txlA* could be detected in either txlXb or txlXg. Both the txlXb and txlXg phenotypes were stable, and their growth on plates and in liquid medium was much faster than that of txlΔNXb. The growth of the txlX strains might be expected to surpass that of txlΔNXb if a truncated TxlA polypeptide synthesized in the txlX strains (which includes the thioredoxin-like region) possesses some TxlA activity. Northern (RNA blot) analysis of RNA from both txlXb and txlXg supports the possibility of the presence of a truncated protein in the txlX mutants. In wild-type cells, a major *txlA*-encoding transcript of about 700 bp is detected, while a truncated *txlA* transcript of about 600 bp (as predicted from the insertion of the Ω cassette at the *Xho*I site) is detected in both of the txlX strains (Fig. 2B).

Physiological analysis. The growth and pigmentation of txlXb and txlXg in liquid medium are summarized in Table 2. The growth rate of txlXg was similar to that of the wild type, but txlXb grew almost 30% more slowly. Whole-cell absorbance spectra were used to monitor the pigmentation of the cells, since the A_{680} reflects Chl content and the A_{620} reflects PC (the major phycobiliprotein component of the PBS) content. The elevated PC/Chl absorbance ratio and blue appear-

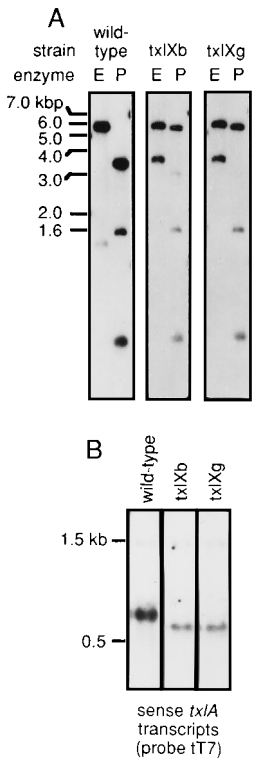

FIG. 2. Analysis of *txlA* DNA and mRNA in mutant strains txlXb and txlXg. (A) Southern blot analysis demonstrating the inactivation of *txlA* in both txlXb and txlXg. Genomic DNA from the wild-type, txlXb, and txlXg strains was digested with either *Eco*RI (lanes E) or *Pst*I (lanes P) and hybridized to a 2.0-kbp probe covering the region containing *txlA* and *nblA* (18). (B) Northern blot analysis of *txlA* transcripts in mRNA isolated from the wild-type, txlXb, and txlXg strains. The probe detects only mRNA encoding TxlA. Equal amounts of rRNA are present in each lane, and the band at 1.5 kb is a nonspecific rRNA signal.

ance of txlXb were the results of a 30% increase in PC content per cell, while cellular Chl content was unchanged. PC content per cell was also elevated 30% in txlXg, but the PC/Chl absorbance ratio appeared wild type because Chl per cell increased by 30% as well. Disruption of TxlA near the C terminus therefore altered the pigmentation of the cells by elevating the PC level in txlXb and by elevating both PC and Chl levels in txlXg. Only the former phenotype was associated with a slow growth rate.

To determine if the additional PC in the txlX strains was assembled into light-harvesting complexes, we isolated and characterized the PBS from the mutants. In wild-type *Synechococcus* sp. strain PCC7942 and in both txlXb and txlXg, virtually all cellular PC was assembled into PBS. The PBS from the mutant strains exhibited a normal size, PC-to-allophycocyanin ratio, polypeptide composition, and physical attachment to the thylakoid membranes. Furthermore, PBS isolated from both txlXb and txlXg exhibited normal fluorescence emission spectra, indicating that energy transfer within the PBS was normal. Finally, the PBS from the mutant strains were shown to be identical to those of the wild type in their susceptibility to proteolysis by trypsin, either when purified or when still attached to the thylakoid membrane. These data (16) demonstrated that the phycobiliproteins and PBS in both txlXb and txlXg were structurally and functionally indistinguishable from those of the wild type and that the increased PC content per cell in the mutants reflected an increased number of apparently normal PBS per cell.

We also examined the energetic connection of the light-harvesting antennae pigments (both PBS and Chl) to the photosynthetic reaction centers by fluorescence emission spectroscopy of whole cells frozen in liquid nitrogen (77 K). As shown in Fig. 3, four main emission peaks are produced when wild-type cells are excited either with 440-nm (absorbed primarily by Chl) or 570-nm (absorbed primarily by PBS) wavelength light. The peak at 650 nm is emitted from PC within the PBS, the peak at 685 nm is due to emissions from both the PBS terminal energy acceptors (at about 680 nm [27, 28]) and the Chl antennae of PSII (CP43, at about 686 nm [22, 33, 49, 52]), the peak at 695 nm is emitted from the PSII reaction center and its CP47 antennae Chl (22, 33, 49, 52), and the peak at 715 nm is emitted from the Chl of PSI (49). In cells excited with 570-nm light, the emission peaks at 650, 685, and 695 nm dominate because PBS transfer energy mainly to PSII (Fig. 3A). In cells excited with 440-nm light, the emission peak at 715 nm is more pronounced because Chl transfers light energy mainly to PSI (Fig. 3B). Also shown are state transitions, which reflect a short-term mechanism for redistributing absorbed light energy between the two reaction centers. If the cells are exposed to light that primarily excites PSI (440 nm) before freezing, relatively more of the absorbed light energy is directed to PSII (state 1; Fig. 3, dark traces). If the cells are exposed to light absorbed primarily by PSII (570 nm) before freezing, relatively more of the absorbed light energy is directed to PSI (state 2; Fig. 3, light traces).

In the mutant txlXg, the state transitions and fluorescence emission spectra appeared normal (Fig. 3E and F). This suggests that despite the increased pigment levels in these cells, the stoichiometry of PSII and PSI, as well as energy transfer between the pigments and photosystems, was normal. Therefore, the reaction centers of both PSII and PSI, along with other components of the photosynthetic apparatus, probably increased proportionately with PBS and Chl in the txlXg mutant. The txlXb mutant also showed relatively normal fluorescence emissions and state transitions when excited with 440-nm

TABLE 2. Growth characteristics[a]

Strain	Mean doubling time (h) ± SD	Mean PC/Chl ratio ± SD	Mean content per cell ± SD	
			PC (10^{-10} mg)	Chl (10^{-11} mg)
Wild type	8.0 ± 0.33 (n = 7), A	1.28 ± 0.04 (n = 19), A	1.33 ± 0.24 (n = 12), A	1.35 ± 0.24 (n = 12), A
txlXb	10.1 ± 0.57 (n = 8), B**	1.55 ± 0.08 (n = 23), B***	1.68 ± 0.2 (n = 15), B**	1.31 ± 0.16 (n = 15), A
txlXg	7.5 ± 0.28 (n = 3), A	1.28 ± 0.03 (n = 10), A	1.75 ± 0.3 (n = 10), B***	1.76 ± 0.26 (n = 10), B**

[a] Cells were grown with 3% CO_2 in air and 50 μmol of photons m^{-2} s^{-1}. The PC/Chl ratio was calculated as $(A_{620} - A_{750})/(A_{680} - A_{750})$. A and B indicate the statistically distinct groups within each column, and the significance of differences from the wild-type values is indicated as follows: *, $P < 0.05$; **, $P < 0.01$; ***, $P < 0.001$.

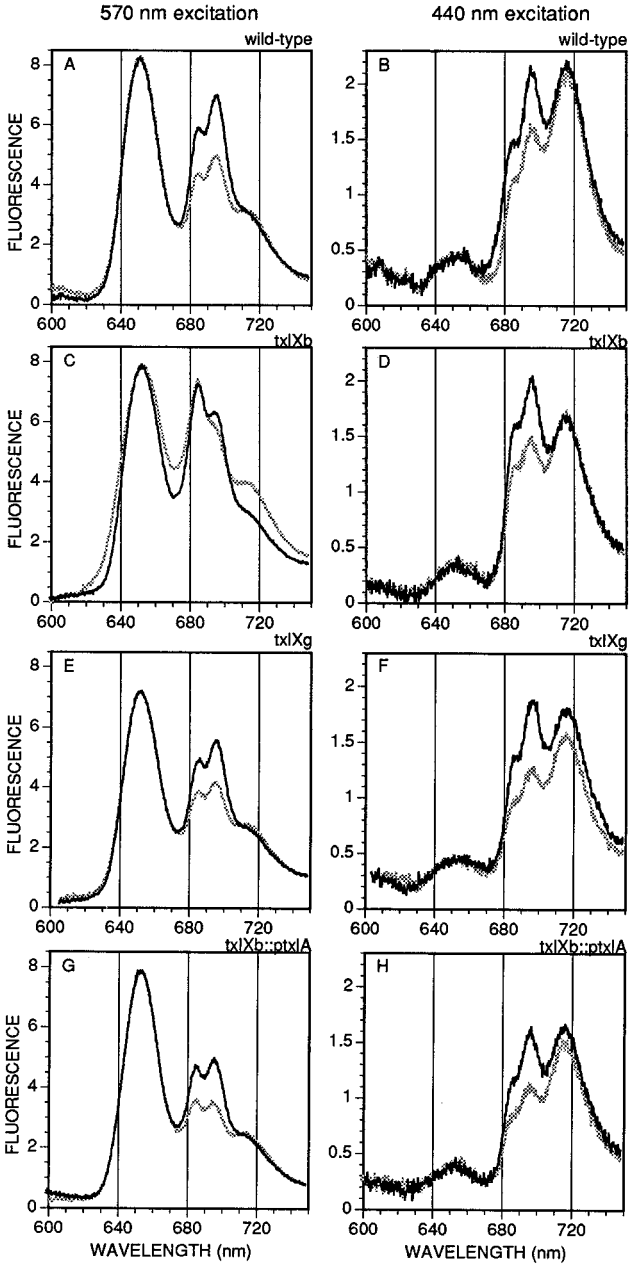

FIG. 3. Fluorescence emission spectra from various strains at 77 K. Spectra from cells pretreated to produce state 1 are shown as dark traces, and spectra from cells pretreated to produce state 2 are shown as light traces. (A) Wild-type cells excited with 570-nm light. (B) Wild-type cells excited with 440-nm light. (C) txlXb excited with 570-nm light. (D) txlXb excited with 440-nm light. (E) txlXg excited with 570-nm light. (F) txlXg excited with 440-nm light. (G) txlXb::ptxlA excited with 570-nm light. (H) txlXb::ptxlA excited with 440-nm light.

light (Fig. 3D; the relative intensity of the PSII and PSI emissions is within the range observed for the wild type). However, when txlXb was excited with 570-nm light (Fig. 3C), the 685-nm peak was much larger relative to the other peaks, and its position was shifted toward the blue end of the spectrum. The positions of this peak were 684.75 ± 0.43 nm ($n = 3$) in wild-type cells, 685.25 ± 0.53 nm ($n = 5$) in txlXg, and 683.45 ± 0.65 nm ($n = 5$) in txlXb. The differences between txlXb and both the wild type and txlXg were statistically significant ($P < 0.05$, Scheffe's f test). Similar changes in the emission maximum near 685 nm have previously been observed when emissions from the PBS terminal energy acceptors (near 680 nm) increase relative to those from PSII antennae Chl (near 686 nm), reflecting a decreased efficiency of energy transfer from the PBS to PSII (21, 30, 58). These data suggest that the excess PBS present in the txlXb strain are not able to transfer harvested light energy to the photosystems. In addition, state transitions were observed in txlXb excited with 570-nm light (Fig. 3C), but in state 2, txlXb showed a relatively greater increase in PSI and smaller decrease in PSII emissions than wild-type cells.

TABLE 3. Rates of O_2 evolution at saturating light intensity (150 μmol of photons m^{-2} s^{-1})[a]

Strain	O_2 evolution per Chl [μmol of O_2 (mg of Chl)$^{-1}$ min^{-1}]	O_2 evolution per cell (10^{11} μmol of O_2 $cell^{-1}$ min^{-1})
Wild type	6.98 (0.59), A	9.42 (0.8), A
txlXb	7.22 (0.26), A	9.46 (0.34), A
txlXg	6.74 (0.07), A	11.86 (0.12), B**

[a] Values are means for three samples (standard deviations). See Table 2, footnote *a*, for definitions of symbols.

The rate of O_2 evolution was used to measure the photosynthetic capacity of PSII in the wild-type and txlX mutant strains. As shown in Table 3, the rates of O_2 evolution on a Chl basis in both txlXb and txlXg were nearly identical to that of wild-type cells. The same was true even at very low light intensities (data not shown). These observations suggest that there were no major differences in the efficiency of PSII or in the stoichiometries of Chl, PSI, and PSII among the strains. However, since txlXg has more Chl per cell, its rate of O_2 evolution per cell was almost 30% higher than that of the wild-type or txlXb strain (Table 3). These data support the suggestion from fluorescence emission spectra that the increased cellular pigmentation of txlXg was accompanied by an increase in the reaction centers and the rest of the photosynthetic apparatus. The elevated photochemical capacity of txlXg per cell might explain why its growth rate is faster than that of txlXb and similar to that of wild-type cells (Table 2).

Reintroduction of intact *txlA*. Table 4 summarizes the characteristics of each strain carrying a normal copy of *txlA* on an autonomously replicating multicopy plasmid (ptxlA; see Materials and Methods). The introduction of *txlA* into wild-type cells (wild-type::ptxlA) had no significant effect on cellular pigmentation or growth rates (Table 4). The introduction of *txlA* into txlXg (txlXg::ptxlA) may have slightly decreased its cellular pigmentation levels, but the effect was not statistically significant (Table 4). In contrast, the introduction of an intact copy of *txlA* into txlXb (txlXb::ptxlA) restored the growth rate, the PC/Chl absorbance ratio (Table 4), and the fluorescence emission spectra (Fig. 3G and H) to those characteristic of the wild type. However, these changes were accomplished not by lowering the cellular PC content to wild-type levels, but by raising the cellular Chl content (Table 4) and rate of O_2 evolution (data not shown) to the levels found in mutant txlXg.

DISCUSSION

The very poor growth of the txlΔNXb mutant suggests that *txlA* plays an important, although perhaps not absolutely essential, role in the metabolism of the cyanobacterium *Synechococcus* sp. strain PCC7942. It is possible that the txlXb and txlXg mutants displayed better growth because the removal of only the C-terminal 34 codons did not prevent TxlA from performing part of its normal function. Hence, the thiore-

TABLE 4. Characteristics of strains carrying plasmid ptxlA[a]

Strain	Mean doubling time (h) ± SD	Mean PC/Chl ratio ± SD	Mean content per cell ± SD	
			PC (10^{-10} mg)	Chl (10^{-11} mg)
Wild type::ptxlA	7.4 ± 0.26 (n = 2), A	1.32 ± 0.03 (n = 6), A	1.29 ± 0.23 (n = 6), A	1.23 ± 0.18 (n = 6), A
txlXb::ptxlA	7.4 ± 0.67 (n = 2), A	1.27 ± 0.03 (n = 6), A	1.79 ± 0.28 (n = 6), B**	1.8 ± 0.28 (n = 6), B**
txlXg::ptxlA	7.3 ± 0.67 (n = 2), A	1.24 ± 0.05 (n = 6), A	1.56 ± 0.23 (n = 6), AB	1.63 ± 0.2 (n = 6), AB

[a] See Table 2, footnote *a*.

doxin-like domain appears crucial to the function of TxlA. Ellis et al. (23) have identified conserved primary and predicted secondary structural motifs that distinguish the enzymes known to function as PDOs from those with weak sequence similarity but no known PDO activity. All of these critical motifs, along with a PDO-like pattern of hydrophobic residues, are found in the thioredoxin-like domain of TxlA. Since TxlA differs in several residues around the active site that are highly conserved among the thioredoxins and is larger than most thioredoxins (although unusually large cyanobacterial "thioredoxins" have been reported [31]), TxlA is unlikely to be a true thioredoxin. Instead, TxlA may function more like the PDIs, which facilitate proper polypeptide folding in the endoplasmic reticulum of eukaryotes and the periplasmic space of bacteria (2, 8, 9, 35, 50, 59), or like a related group of PDOs involved in cytochrome biosynthesis in the periplasm of bacteria (10, 39). By analogy to the PDIs, the active site of TxlA might be located either in the periplasm or the thylakoid lumen, but the possibility of a cytosolic location for the TxlA active site (as in thioredoxins) has not been excluded.

Interruption of *txlA* by construct txlX generated two mutant strains, designated txlXb and txlXg, with distinct phenotypes. Both strains synthesized truncated *txlA* mRNA (Fig. 2B) and probably produced a truncated TxlA polypeptide. Both of the mutants also exhibited an increase in cellular PBS content (Table 2); however, the PBS structure appeared to be unaffected by the mutation. In txlXb, the excess PBS were not able to efficiently transfer harvested light energy to the photosynthetic reaction centers (Fig. 3). In txlXg, the increase in cellular PBS content was accompanied by a proportionate increase in levels of Chl, reaction centers, and probably other components of the photosynthetic apparatus, with which the "excess" PBS were functionally integrated (Fig. 3, Table 3). Intact *txlA* was unable to restore the parental phenotype to either of these mutants (Table 4). In fact, the presence of full-length TxlA in the txlXb strain converted it to the phenotype of txlXg. One possible explanation for these results is that the interaction of truncated and full-length TxlA polypeptides in the txlXb::ptxlA strain produced a similar effect as when the truncated TxlA polypeptide interacted with another protein in mutant txlXg. Both the txlXb and txlXg phenotypes could result from the same mutation in *txlA* if this second protein differed between the two strains. Since the frequencies of both the txlXb and txlXg phenotypes are relatively high (80 and 20% of the double homologous recombinants, respectively), it is not likely that either is the consequence of a spontaneous mutation occurring after disruption of *txlA*. It is more likely that the putative second-site locus was polymorphic in the original population of mutagenized cells. Since each cyanobacterial cell carries multiple copies of the chromosome, it is also possible that such a polymorphism could reside within a single cell.

The phenotypes of the txlX mutants show that the C-terminal domain is important for some aspect of TxlA's role in the cell. It is possible that the disruption of *txlA* in the txlX strains was directly responsible for the production of excess PBS and that the slow growth of txlXb simply reflected the diversion of resources from growth into the production of excess PBS. The proportionate increase in cellular photosynthetic capacity observed in txlXg might then provide the extra biosynthetic capacity needed to attain a normal growth rate despite the higher PBS content. However, the growth rates of the wild-type, txlXb, and txlXg strains under carbon-limited conditions (i.e., during growth on air instead of air enriched with 3% CO_2) were indistinguishable (doubling time approximately 14 h; data not shown). The rates of O_2 evolution in the wild-type and txlXb strains during carbon-limited growth were also indistinguishable [approximately 5.5 μmol of O_2 (mg of Chl)$^{-1}$ min^{-1}]. Under these conditions, txlXb still had normal levels of Chl per cell, elevated levels of PC per cell, and abnormal fluorescence emission spectra (data not shown). Therefore, the production of excess PBS did not slow the growth of txlXb on air unsupplemented with CO_2, making it seem unlikely that the expenditure of energy required to synthesize excess PBS was alone responsible for retarding its growth on CO_2-enriched air.

It is possible that the changes in cellular pigmentation observed in the txlX mutants are indirect, occurring in response to an underlying change in cellular metabolism. The observation that txlXb does not grow more slowly than the wild type on air that is not enriched with CO_2 suggests that txlXb is unable to adjust its metabolism to match the faster growth rate of the wild type under carbon-rich conditions. This could reflect a number of defects, such as improper regulation of carbon metabolism or an inability to properly modulate the pathways of photosynthetic electron transport, which differ during carbon-limited and carbon-rich growth. The similarity of TxlA to thioredoxins and other PDOs also suggests that it could play a role in the synthesis, monitoring, or redox regulation of electron transport pathways. If disruption of *txlA* perturbed the normal flow of electrons, cyanobacteria might respond by adjusting the photosynthetic apparatus, just as they modulate the structure and function of the photosynthetic apparatus to suit the metabolic demands of different environmental conditions (see the introduction). An even more direct link between TxlA and the regulation of the cyanobacterial photosynthetic apparatus may be implied if the antisense *txlA* mRNA produced in nutrient-deprived *Synechococcus* sp. strain PCC7942 cells is found to regulate TxlA expression (16, 18).

While these data do not allow us to precisely define the function of *txlA*, they strongly suggest that TxlA can influence the structure and function of the cyanobacterial photosynthetic apparatus. Further physiological and biochemical characterization of TxlA, txlXb, and txlXg not only should reveal the function of TxlA, but may also provide new molecular insights into the regulation of the cyanobacterial photosynthetic apparatus.

ACKNOWLEDGMENTS

We thank Glenn Ford for helping in the maintenance and operation of the equipment used in these studies. Dave Fork kindly provided access to and assistance with both the fluorometer and the O_2 electrode. Jane Edwards helped in the preparation of the manuscript. John Davies, Steve Herbert, Dave Kehoe, Fitnat Yildiz, Devaki Bhaya, and other members of the laboratory have been very helpful in discussing this work and its interpretation.

This work was supported by USDA grant 94-37306-0344 awarded to A.R.G. and the Carnegie Institution of Washington. J.L.C. was supported by NIH CMB training grant 5T32GM07276.

REFERENCES

1. **Aizawa, K., T. Shimizu, T. Hiyama, K. Satoh, Y. Nakamura, and Y. Fujita.** 1992. Changes in composition of membrane proteins accompanying the regulation of PS I/PS II stoichiometry observed with *Synechocystis* PCC 6803. Photosyn. Res. **32:**131–138.
2. **Akiyama, Y., S. Kamitani, N. Kusukawa, and K. Ito.** 1992. *In vitro* catalysis of oxidative folding of disulfide-bonded proteins by the *Escherichia coli dsbA* (*ppfA*) gene product. J. Biol. Chem. **267:**22440–22445.
3. **Allen, J. F.** 1992. Protein phosphorylation in regulation of photosynthesis. Biochim. Biophys. Acta **1098:**275–335.
4. **Allen, J. F.** 1993. Redox control of gene expression and the function of chloroplast genomes—an hypothesis. Photosyn. Res. **36:**95–102.
5. **Allen, M. M.** 1969. Simple conditions for the growth of unicellular blue-green algae on plates. J. Phycol. **4:**1–3.
6. **Arnon, D. I., B. D. McSwain, H. Y. Tsujimoto, and K. Wada.** 1974. Photochemical activity and components of membrane preparations from blue-green algae. I. Coexistence of two photosystems in relation to chlorophyll *a* and removal of phycocyanin. Biochim. Biophys. Acta **357:**231–245.
7. **Ausubel, F. M., R. Brent, R. E. Kingston, D. D. Moore, J. G. Seidman, J. A. Smith, and K. Struhl.** 1988. Current protocols in molecular biology. John Wiley and Sons, New York.
8. **Bardwell, J. C. A., and J. Beckwith.** 1993. The bonds that tie: catalyzed disulfide bond formation. Cell **74:**769–771.
9. **Bardwell, J. C. A., K. McGovern, and J. Beckwith.** 1991. Identification of a protein required for disulfide bond formation in vivo. Cell **67:**581–589.
10. **Beckman, D. L., and R. G. Kranz.** 1993. Cytochrome *c* biogenesis in a photosynthetic bacterium requires a periplasmic thioredoxin-like protein. Proc. Natl. Acad. Sci. USA **90:**2179–2183.
11. **Belknap, W. R., and R. Haselkorn.** 1987. Cloning and light regulation of expression of the phycocyanin operon of the cyanobacterium *Anabaena*. EMBO J. **6:**871–884.
12. **Blankenship, R. E., P. Cheng, T. P. Causgrove, D. C. Brune, S. H.-H. Wang, J.-U. Choh, and J. Wang.** 1993. Redox regulation of energy transfer efficiency in antennas of green photosynthetic bacteria. Photochem. Photobiol. **57:**103–107.
13. **Bruce, D., and O. Salehian.** 1992. Laser-induced optoacoustic calorimetry of cyanobacteria: the efficiency of primary photosynthetic processes in state 1 and state 2. Biochim. Biophys. Acta **1100:**242–250.
14. **Buchanan, B. B.** 1991. Regulation of CO_2 assimilation in oxygenic photosynthesis: the ferredoxin/thioredoxin system. Arch. Biochem. Biophys. **288:** 1–9.
15. **Campbell, D., J. Houmard, and N. Tandeau de Marsac.** 1993. Electron transport regulates cellular differentiation in the filamentous cyanobacterium *Calothrix*. Plant Cell **5:**451–463.
16. **Collier, J. L.** 1994. Molecular genetic and physiological investigations into the acclimation of the cyanobacterial photosynthetic apparatus to nutrient deprivation. Ph. D. thesis, Stanford University, Stanford, Calif.
17. **Collier, J. L., and A. R. Grossman.** 1992. Chlorosis induced by nutrient deprivation in *Synechococcus* sp. strain PCC 7942: not all bleaching is the same. J. Bacteriol. **174:**4718–4726.
18. **Collier, J. L., and A. R. Grossman.** 1994. A small polypeptide triggers complete degradation of light-harvesting phycobilisomes in nutrient-deprived cyanobacteria. EMBO J. **13:**1039–1047.
19. **Collier, J. L., S. K. Herbert, D. C. Fork, and A. R. Grossman.** Changes in the cyanobacterial photosynthetic apparatus in response to macronutrient deprivation. Photosyn. Res. **42:**173–183.
20. **de Lorimier, R. M., R. L. Smith, and S. E. Stevens, Jr.** 1992. Regulation of phycobilisome structure and gene expression by light intensity. Plant Physiol. **98:**1003–1010.
21. **Döhler, G., and K.-R. Pryzbylla.** 1970. Untersuchung der Beziehung zwischen Pigmentzusammensetzung und CO_2-Gaswechsel bei der Blaualge *Anacystis nidulans*. Planta **90:**163–173.
22. **Dzelzkalns, V. A., and L. Bogorad.** 1989. Spectral properties and composition of reaction center and ancillary polypeptide complexes of photosystem II deficient mutants of *Synechocystis* 6803. Plant Physiol. **90:**617–623.
23. **Ellis, L. B. M., P. Saurugger, and C. Woodward.** 1992. Identification of the three-dimensional thioredoxin motif: related structure in the ORF3 protein of the *Staphylococcus aureus mer* operon. Biochemistry **31:**4882–4891.
24. **Fork, D. C., and S. K. Herbert.** 1993. Electron transport and photophosphorylation by photosystem I in vivo in plants and cyanobacteria. Photosyn. Res. **36:**149–168.
25. **Fujita, Y., A. Murakami, and K. Ohki.** 1987. Regulation of photosystem composition in the cyanobacterial photosynthetic system: the regulation occurs in response to the redox state of the electron pool located between the two photosystems. Plant Cell Physiol. **28:**283–292.
26. **Fujita, Y., K. Ohki, and A. Murakami.** 1985. Chromatic regulation of photosystem composition in the photosynthetic systems of red and blue-green algae. Plant Cell Physiol. **26:**1541–1548.
27. **Gantt, E., and C. A. Lipschultz.** 1973. Energy transfer in phycobilisomes from phycoerythrin to allophycocyanin. Biochim. Biophys. Acta **292:**858–861.
28. **Gantt, E., C. A. Lipschultz, J. Grabowski, and B. K. Zimmerman.** 1979. Phycobilisomes from blue-green and red algae: isolation criteria and dissociation characteristics. Plant Physiol. **63:**615–620.
29. **Gendel, S., N. Straus, D. Pulleybank, and J. Williams.** 1983. Shuttle cloning vectors for the cyanobacterium *Anacystis nidulans*. J. Bacteriol. **156:**148–154.
30. **Ghosh, A. K., and Govindjee.** 1966. Transfer of the excitation energy in *Anacystis nidulans* grown to obtain different pigment ratios. Biophys. J. **6:**611–619.
31. **Gleason, F. K.** 1992. Activities of two dissimilar thioredoxins from the cyanobacterium *Anabaena* sp. strain PCC 7120. J. Bacteriol. **174:**2592–2598.
32. **Grossman, A. R., M. R. Schaefer, G. G. Chiang, and J. L. Collier.** 1993. The phycobilisome, a light-harvesting complex responsive to environmental conditions. Microbiol. Rev. **57:**725–749.
33. **Haag, E., J. J. Eaton-Rye, G. Renger, and W. F. J. Vermaas.** 1993. Functionally important domains of the large hydrophilic loop of CP47 as probed by oligonucleotide-directed mutagenesis in *Synechocystis* sp. PCC 6803. Biochemistry **32:**4444–4454.
34. **Herbert, S. K., D. C. Fork, and S. Malkin.** 1990. Photoacoustic measurements *in vivo* of energy storage by cyclic electron flow in algae and higher plants. Plant Physiol. **94:**926–934.
35. **Kamitani, S., Y. Akiyama, and K. Ito.** 1992. Identification and characterization of an *Escherichia coli* gene required for the formation of correctly folded alkaline phosphatase, a periplasmic enzyme. EMBO J. **11:**57–62.
36. **Kaplan, A., R. Schwarz, J. Lieman-Hurwitz, and L. Reinhold.** 1991. Physiological and molecular aspects of the inorganic carbon-concentrating mechanism in cyanobacteria. Plant Physiol. **97:**851–855.
37. **Kim, J. H., R. E. Glick, and A. Melis.** 1993. Dynamics of photosystem stoichiometry adjustment by light quality in chloroplasts. Plant Physiol. **102:** 181–190.
38. **Laudenbach, D. E., and A. R. Grossman.** 1991. Characterization and mutagenesis of sulfur-regulated genes in a cyanobacterium: evidence for function in sulfate transport. J. Bacteriol. **173:**2739–2750.
39. **Loferer, H., M. Bott, and H. Hennecke.** 1993. *Bradyrhizobium japonicum* TlpA, a novel membrane-anchored thioredoxin-like protein involved in the biogenesis of cytochrome aa_3 and in development of symbiosis. EMBO J. **12:**3373–3383.
40. **Lönneborg, A., L. K. Lind, S. R. Kalla, P. Gustafsson, and G. Öquist.** 1985. Acclimation processes in the light-harvesting system of the cyanobacterium *Anacystis nidulans* following a light shift from white to red. Plant Physiol. **78:**110–114.
41. **Maeda, H., and T. Watanabe.** 1992. Assay of photosynthetic reaction centers by HPLC quantitation of chlorophyll *a'* and pheophytin *a*: application to the chromatic regulation of photosystem stoichiometry in cyanophytes. J. Photochem. Photobiol. B Biol. **13:**267–274.
42. **Manodori, A., M. Alhadeff, A. N. Glazer, and A. Melis.** 1984. Photochemical apparatus organization in *Synechococcus* 6301 (*Anacystis nidulans*): effect of phycobilisome mutation. Arch. Microbiol. **139:**117–123.
43. **Manodori, A., and A. Melis.** 1986. Cyanobacterial acclimation to photosystem I or photosystem II light. Plant Physiol. **82:**185–189.
44. **Manodori, A., and A. Melis.** 1986. Light quality regulates photosystem stoichiometry in cyanobacteria, p. 653–662. *In* G. Akoyunoglou and H. Senger (ed.), Regulation of chloroplast differentiation. Alan R. Liss, New York.
45. **Manodori, A., and A. Melis.** 1984. Photochemical apparatus organization in *Anacystis nidulans* (Cyanophyceae): effect of CO_2 concentration during cell growth. Plant Physiol. **74:**67–71.
46. **Muller, E. G. D., and B. B. Buchanan.** 1989. Thioredoxin is essential for photosynthetic growth: the thioredoxin *m* gene of *Anacystis nidulans*. J. Biol. Chem. **264:**4008–4014.
47. **Mullineaux, C. W.** 1992. Excitation energy transfer from phycobilisomes to photosystem I in a cyanobacterium. Biochim. Biophys. Acta **1100:**285–292.
48. **Murakami, A., and Y. Fujita.** 1991. Regulation of photosystem stoichiometry in the photosynthetic system of the cyanophyte *Synechocystis* PCC 6714 in response to light intensity. Plant Cell Physiol. **32:**223–230.
49. **Nilsson, F., D. J. Simpson, C. Jansson, and B. Andersson.** 1992. Ultrastructural and biochemical characterization of a *Synechocystis* 6803 mutant with inactivated *psbA* genes. Arch. Biochem. Biophys. **295:**340–347.
50. **Noiva, R., and W. J. Lennarz.** 1992. Protein disulfide isomerase: a multifunctional protein resident in the lumen of the endoplasmic reticulum. J. Biol. Chem. **267:**3553–3556.

51. **Ogawa, T.** 1992. Identification and characterization of the *ictA*/*ndhL* gene product essential to inorganic carbon transport of *Synechocystis* PCC6803. Plant Physiol. **99:**1604–1608.
52. **Pakrasi, H. B., H. C. Reithman, and L. A. Sherman.** 1985. Organization of pigment proteins in the photosystem II complex of the cyanobacterium *Anacystis nidulans* R2. Proc. Natl. Acad. Sci. USA **82:**6903–6907.
53. **Pierce, J., and T. Omata.** 1988. Uptake and utilization of inorganic carbon by cyanobacteria. Photosyn. Res. **16:**141–154.
54. **Prentki, P., and H. M. Krisch.** 1984. In vitro insertional mutagenesis with a selectable DNA fragment. Gene **29:**303–313.
55. **Sambrook, J., E. F. Fritsch, and T. Maniatis.** 1989. Molecular cloning: a laboratory manual, 2nd ed. Cold Spring Harbor Laboratory Press, Cold Spring Harbor, N.Y.
56. **Tsinoremas, N. F., A. M. Castets, M. A. Harrison, J. F. Allen, and N. Tandeau de Marsac.** 1991. Photosynthetic electron transport controls nitrogen assimilation in cyanobacteria by means of posttranslational modification of the *glnB* gene product. Proc. Natl. Acad. Sci. USA **88:**4565–4569.
57. **Vernotte, C., C. Astier, and J. Olive.** 1990. State 1-state 2 adaptation in the cyanobacteria *Synechocystis* PCC 6714 wild type and *Synechocystis* PCC 6803 wild type and phycocyanin-less mutant. Photosyn. Res. **26:**203–212.
58. **Vernotte, C., M. Picaud, D. Kirilovsky, J. Olive, G. Ajlani, and C. Astier.** 1992. Changes in the photosynthetic apparatus in the cyanobacterium *Synechocystis* sp. PCC 6714 following light-to-dark and dark-to-light transitions. Photosyn. Res. **32:**45–57.
59. **Yu, J., S. McLaughlin, R. B. Freedman, and T. R. Hirst.** 1993. Cloning and active site mutagenesis of *Vibrio cholerae* DsbA, a periplasmic enzyme that catalyzes disulfide bond formation. J. Biol. Chem. **268:**4326–4330.